Journal of Sound and Vibration (1997) **202**(3), 375–394

A HYBRID ENERGY METHOD FOR PREDICTING HIGH FREQUENCY VIBRATIONAL RESPONSE OF POINT-LOADED PLATES

M. J. SMITH

Martec Limited, Suite 400 1888 *Brunswick St, Halifax NS, Canada B3J* 3J8

(*Received* 28 *May* 1996 *and in final form* 28 *October* 1996)

Modelling of the far-field energy distribution and power flow in point-loaded finite plates is considered. First, the two-dimensional conductivity equation governing the energy distribution in a plate is derived from fundamental energy and intensity considerations. The derivation, previously unreported, illustrates the basic assumptions and limitations of the conductivity method. A hybrid model is then developed in which contributions to the direct and reverberant fields are estimated separately. The direct field component is approximated by the far-field response of an infinite plate; the reverberant contribution is governed by a homogenous conductivity equation with a reflected power distribution along the boundary of the plate. The partition of power between the direct and reverberant fields is approximated by assuming a circular plate with an equivalent surface area. The method is found to be effective for predicting the spatial variation in the response when both the direct and reverberant fields participate strongly, a case not well predicted by statistical energy analysis, or by the conductivity method. The method is applied to examples of a centrally loaded square plate, and a rectangular plate with two uncorrelated point loads.

1. INTRODUCTION

The vibrational conductivity method has emerged in recent years as a competitor to statistical energy analysis (SEA) in the field of high frequency structural response prediction. Relevant applications are noise propagation analysis and passive noise control design of automobile, ship, and aerospace structures.

The vibrational conductivity method is founded on an analogy between the time-averaged flow of vibrational energy in a structural element and the flow of the thermal energy in a one- or two-dimensional region. The basic equations are in the form of heat conduction laws, and can be solved with a variety of analytical and numerical methods. Among the advantages over SEA that have been cited are the following: (1) A greater modelling flexibility in so far as existing FE models of structural components can be applied directly to high frequency analysis, and in its ability to model non-uniform distributions of damping materials which may be applied for purpose of noise control; (2) the ability to predict a spatially varying vibration level across a structural component, as opposed to the single response value given by SEA; and (3) a more accurate visualization of the energy flow in a system, enabling better design and control of noise propagation and structural response. The method has been used successfully with frame models, including those with more than one mode of energy transmission [1–3].

The two-dimensional conductivity equation was first applied to plate structures by Buvailo and Ionov [4], in a finite element formulation of the problem. The theoretical

0022–460X/97/180375 + 20 $25.00/0/sv960833

validity of the method for plates and membranes was more firmly established by Bouthier [5], who showed that the two-dimensional conductivity equation required an assumption of plane-wave energy propagation, and a time-averaged and locally space-averaged energy density. A further finite element formulation was given by Bouthier and Bernhard [6], and numerous examples of the method applied to finite plates and membranes were also presented by these authors [7, 8]. Recently, Bernhard and Huff [9, 10] have demonstrated the use of the technique with systems of interconnected plates.

Energy modelling of circular plates was addressed by Burrell *et al*. [11] and Kim *et al*. [12]. It was shown that the energy distribution over such plates with central point loading do not obey the two-dimensional conductivity equation; instead, it is governed by a one-dimensional equation of second order. If the circular plate extends to infinity, this equation reduces to a first order equation which is not of conductivity form. The differences in the modelling are a consequence of the physical behaviour of the respective systems. The wave field on an infinite or circular plate consists of cylindrical waves concentric with the driving point; whereas on a rectangular plate in which numerous reflections from the boundaries occur, the wave field is effectively diffuse, and can often be approximated by a field of randomly oriented plane waves. This accounts for the successful application of the conductivity equation by Bouthier to plates and membranes with predominantly reverberant wave fields.

But when the dynamic response shows significant spatial variation, the conductivity equation is unsuitable for point excited plates, as was pointed out in a recent study by Langley [13]. This generally occurs with heavily damped or short wavelength vibration. Moreover, the response with light damping or long wavelength oscillation is essentially flat, and therefore would be well predicted by SEA; it is therefore the spatially varying case which is of particular interest in establishing the validity of the conductivity method.

The lack of a suitable model for all types of plate excitation and response has hindered the acceptance of the conductivity method, and has led to the belief that the conductivity equations are merely an analogy without mathematical foundation [14]. Some confusion also seems to have been generated regarding the correct interpretation of the energy terms used in the equations. These are often derived in the context of harmonic excitation, but are then applied to broadband noise excitation without explanation. Furthermore, the conductivity equation derived by Nefkse and Sung [1] for beams emphasizes the use of time-averaged energy density, whereas the derivation for plates given by Bouthier uses a time- and space-averaged energy density. Various other attempts have been made at energy modelling. Lase and Jezequel [15] have presented a more exact formulation of the energy distribution in beams, but solutions to the equations are not easily obtained. Carcaterra and Sestieri [14] have derived the general dynamical equations of an elastic body in terms of the time-averaged kinetic energy, and have shown that conductivity-type equations are not forthcoming from this change of variables.

The present study is an attempt to resolve some of the difficulties involved in applying the conductivity method to plates. Particular attention is given to point-excited plates with finite dimensions. The two-dimensional conductivity equation is derived from fundamental energy and intensity considerations, thereby complementing a derivation arising from the classical plate equation given previously by Bouthier [5]. It is noted that the energy distributions in direct and reverberant fields are governed by different equations. The standard conductivity equation is only applicable to the reverberant portion of the energy; whereas the equation governing a point-loaded infinite plate is only applicable to the portion of plate energy flowing directly from the excitation. A hybrid modelling approach for finite plates is presented in which the contributions to the direct and reverberant fields are determined independently. The method is then illustrated for a pair of example plates.

2. CONDUCTIVITY EQUATION FOR TWO-DIMENSIONAL DIFFUSE FIELDS

In this section a derivation of the two-dimensional conductivity equation is given. The derivation follows the approach taken by Nefske and Sung [1] for beams, and is generalized for two-dimensional wave fields. In the development of expressions and intensity, only far-field waves are considered: near-fields and boundary effects are neglected.

Three important properties of energy and intensity must be established before conductivity modelling can be pursued. First consider one-dimensional propagation of flexural plane waves on a plate in which only forward and backward propagating wave components travel in directions **r** and **-r**, respectively. The time-averaged intensity is a vector quantity defined as the rate at which energy travels across a unit width running perpendicular to the direction of propagation. The intensity in the two wave components can be expressed as [16]

$$\langle \mathbf{q}^+ \rangle = c\langle e^+ \rangle \mathbf{r}, \qquad \langle \mathbf{q}^- \rangle = -c\langle e^- \rangle \mathbf{r}, \tag{1}$$

where c is the group velocity, $\langle \mathbf{q}^+ \rangle$ and $\langle \mathbf{q}^- \rangle$ are the time-averaged intensities, and $\langle e^+ \rangle$ and $\langle e^- \rangle$ are the time-averaged energy densities in forward and backward travelling waves, respectively. The time-averaging, indicated by the angle brackets, is performed over a duration of one period of oscillation.

Noiseux [17] showed that in the absence of damping, the net intensity $\langle \mathbf{q} \rangle$ is constant and equal to the vector sum of the oppositely directed intensities of the two travelling waves:

$$\langle \mathbf{q} \rangle = \langle \mathbf{q}^+ \rangle + \langle \mathbf{q}^- \rangle. \tag{2}$$

This equation also holds for light damping, in which $\langle \mathbf{q} \rangle$ is subject to spatial variation.

The third property relates the total vibrational energy density to the energy densities of the component waves. Wohlever and Bernhard [2] have shown that for dispersive wave types such as flexural waves, a simple relation exists only when the energy densities are both time-averaged and locally space-averaged. The total energy is the sum of the time-averaged energy components:

$$\overline{\langle e \rangle} = \langle e^+ \rangle + \langle e^- \rangle, \tag{3}$$

where local space-averaging is indicated with a bar. The space-average is local in the sense that the net energy at a particular location need only be averaged over one-half wavelength in the direction of propagation. Note that the energies of the wave components are only time-averaged. The time-average, in addition to removing the time-variation in the quantities, allows the energy densities to be expressed as twice their respective time-averaged kinetic energy densities, thus enabling calculated energy distributions to be directly converted to dynamic response distributions.

Although equations (1)–(3) are derived for harmonic wave fields, they equally apply to one-dimensional wave fields made up of a superposition of multiple frequency waves and also to the case of random noise fields [17]. The independence of the energies and intensities of the participating wave components allows broadband noise and multitonal cases to be analyzed in the same way as harmonic fields.

The time rate of change of the energy density can be shown to obey the relation

$$\frac{\partial \overline{\langle e \rangle}}{\partial t} = \nabla \cdot \langle \mathbf{q} \rangle + \pi_d - \pi_i, \tag{4}$$

where $\langle \mathbf{q} \rangle = \langle q_x \rangle \mathbf{i} + \langle q_y \rangle \mathbf{j}$ is the intensity vector, π_d is the power dissipated per unit area and π_i is the external power input per unit area. This equation is obtained by considering the energy balance in a differential area of plate, and holds regardless of the nature of the wave field. With harmonic waves of frequency ω and hysteretic loss factor of η, the average energy dissipation rate is [16]

$$\pi_d = \omega \eta \overline{\langle e \rangle}. \tag{5}$$

Alternatively, if the vibrational energy is made up of multiple frequency or broadband random noise components, ω can be replaced with an average, or centre frequency.

The energy balance equation (4) governing the net energy and intensity also governs the energy and intensity of individual components, as can be verified by superposition. Of interest to high frequency vibration is the steady-state case in which the left-side of equation (4) is set to zero. For a plane wave travelling in a direction defined by the unit vector $\mathbf{r}$ with frequency ω and intensity $\langle \mathbf{q}^+ \rangle$, putting $\pi_i = 0$ in equation (4) gives

$$\nabla \cdot \langle \mathbf{q}^+ \rangle = -\omega \eta \langle e^+ \rangle, \tag{6}$$

where $\langle e^+ \rangle$ is the energy density of the component travelling in direction $\mathbf{r}$. A similar wave travelling in direction $-\mathbf{r}$ with intensity $\langle \mathbf{q}^- \rangle$ will obey equation

$$\nabla \cdot \langle \mathbf{q}^- \rangle = -\omega \eta \langle e^- \rangle, \tag{7}$$

where $\langle e^- \rangle$ is the energy density of the component travelling in the direction $-\mathbf{r}$.

Subtracting equation (7) from equation (6) gives the following result:

$$\partial/\partial x \, (\langle q_x^+ \rangle - \langle q_x^- \rangle) + \partial/\partial y (\langle q_y^+ \rangle - \langle q_y^- \rangle) = -\omega \eta (\langle e^+ \rangle - \langle e^- \rangle). \tag{8}$$

The energy densities on the right hand side of this equation are related to the magnitudes of the intensity components by equation (1). With $\mathbf{r} = \cos\theta \mathbf{i} + \sin\theta \mathbf{j}$, the x and y components of the intensities are given by

$$\langle q_x^+ \rangle = c \langle e^+ \rangle \cos\theta, \qquad \langle q_x^- \rangle = -c \langle e^- \rangle \cos\theta, \qquad \langle q_y^+ \rangle = c \langle e^+ \rangle \sin\theta,$$
$$\langle q_y^- \rangle = -c \langle e^- \rangle \sin\theta. \tag{9}$$

and the magnitudes of the intensities are given by

$$\langle \mathbf{q}^+ \rangle \cdot \mathbf{r} = c \langle e^+ \rangle, \qquad \langle \mathbf{q}^- \rangle \cdot (-\mathbf{r}) = c \langle e^- \rangle. \tag{10}$$

Substituting equation (9) into the left side and equation (10) into the right side of equation (8), the following expression is obtained:

$$\{\cos\theta(\partial/\partial x) + \sin\theta(\partial/\partial y)\} c (\langle e^+ \rangle + \langle e^- \rangle) = -(\omega\eta/c)(\langle \mathbf{q}^+ \rangle + \langle \mathbf{q}^- \rangle) \cdot \mathbf{r}. \tag{11}$$

Applying equations (2) and (3), and recognizing the left side as the magnitude of a gradient in direction $\mathbf{r}$, equation (11) reduces to

$$[\nabla(c\overline{\langle e \rangle}) + (\omega\eta/c)\langle \mathbf{q} \rangle] \cdot \mathbf{r} = 0. \tag{12}$$

If the plate is isotropic so that c is the same in all directions, the direction of propagation $\mathbf{r}$ can be considered arbitrary. Thus the term inside the square brackets must equal zero irrespective of $\mathbf{r}$, giving the net intensity as

$$\langle \mathbf{q} \rangle = -(c/\omega\eta) \, \nabla(c\overline{\langle e \rangle}). \tag{13}$$

This result is analogous to Fourier's law for heat conduction, and indicates that energy flows from regions of high energy to regions of low energy in a direction opposite to the local gradient.

The final step is to substitute equation (13) back into equation (4), whereupon the following result is obtained:

$$\frac{\partial}{\partial x}\left(\frac{c}{\omega\eta}\frac{\partial}{\partial x}(c\overline{\langle e\rangle})\right)+\frac{\partial}{\partial y}\left(\frac{c}{\omega\eta}\frac{\partial}{\partial y}(c\overline{\langle e\rangle})\right)-\omega\eta\overline{\langle e\rangle}=-\pi_i. \tag{14}$$

If c and η are constants over the area of the plate, the equation simplifies to

$$(c^2/\omega\eta)\,\nabla^2\overline{\langle e\rangle}-\omega\eta\overline{\langle e\rangle}=-\pi_i. \tag{15}$$

Since equations (1)–(4) apply to broadband as well as harmonic plane waves, there is no obstacle in extending the application of equations (13) and (15) to a plane broadband disturbance with a mean frequency of ω.

Now consider a diffuse field comprised of uncorrelated, randomly-directed plane harmonic waves or plane broadband disturbances. The total energy density in the diffuse field can be expressed as the sum of the energies in each of the plane wave components:

$$\overline{\langle e\rangle}_{diffuse}=\sum_j\overline{\langle e\rangle}_j, \tag{16}$$

where $\overline{\langle e\rangle}_j$ is the average energy density in a plane wave component. This follows from recognizing that phase interactions between plane waves travelling in different directions will disappear under time- and local space-averaging. Likewise, the net intensity in the diffuse field is, in the time- and space-averaged sense, equal to the sum of the component intensities:

$$\overline{\langle\mathbf{q}\rangle}_{diffuse}=\sum_j\langle\mathbf{q}\rangle_j=-\sum_j(c/\omega\eta)\,\nabla(c\overline{\langle e\rangle}_j)=-(c/\omega\eta)\,\nabla(c\overline{\langle e\rangle}_{diffuse}). \tag{17}$$

Thus the intensity in a diffuse field obeys the same Fourier's law expression as each of the plane wave components.

Again assuming steady state conditions, the intensity expression (17) is now substituted into the general energy balance equation (4). With a dissipation function for the diffuse field of the same form as equation (5), a conductivity equation identical to equation (15) is obtained, but where the energy density $\overline{\langle e\rangle}$ now refers to that of the diffuse field. This generalization of equation (15) is the result of the linearity of the equations, and the mutual independence of the individual energy components. But the assumption of plane waves or plane broadband disturbances cannot be abandoned in this generalization since both equations (13) and (17) depend on it. Thus the conductivity equation (15) cannot be used to describe the energy in the direct field produced by a point excitation, as this field cannot be represented by superposition of plane waves.

Because equation (15) is a second-order differential equation, it requires just one boundary condition at all points on the plate edge which must be expressible as a combination of zeroth and first order spatial derivatives of the energy density. For plates of finite size with clamped or simply supported edges, two candidate boundary conditions may be considered. A zero edge velocity implies a zero energy density along the boundary:

$$\overline{\langle e\rangle}|_\Gamma=0, \tag{18}$$

where Γ denotes the boundary. Alternatively, a clamped or simply supported edge can be considered perfectly reflecting so that the net intensity normal to the boundary is zero:

$$\overline{\langle \mathbf{q} \rangle}|_\Gamma \cdot \mathbf{n} = -(c/\omega\eta)\, \nabla(c\overline{\langle e \rangle})|_\Gamma \cdot \mathbf{n} = 0, \tag{19}$$

where n is the outwardly directed unit normal. Note that this last boundary condition could also be used for a free edge.

In the high frequency limit the nature of the edge constraint should have only a marginal effect on the energy distribution. It is therefore appropriate to use equation (19) since it applies to a wider range of edge constraints. The boundary condition can be further generalized by including a normally-directed intensity distribution for situations where an energy flow across the edge is permissible. The latter may include edge excitations or damping, or a flow across the boundary to an adjacent component.

3. ENERGY DISTRIBUTIONS IN POINT-LOADED PLATES

Bouthier [5] and others have given numerous examples of the use of equation (15) for determining the dynamic response of plates to harmonic or broadband excitations. Zero normal intensity is usually assumed on the boundaries, and solutions have been obtained with Fourier series expansions or by finite element discretization. The power input to the plate is determined from force magnitudes and driving point impedances.

For harmonic point loading, the conductivity equation has been found to predict the energy distribution, and hence the dynamic response, with reasonable accuracy under certain conditions. In cases of lightly damped or relatively long wavelength vibration, the diffuse equation (15) gives a nearly uniform response across the plate, representing a smooth, locally space-averaged version of the exact standing wave field. The accuracy of this response level depends on correct estimation of the input power at a particular frequency. The results given by Bouthier [5] use input powers derived from the exact driving point impedance at the frequency of excitation. This enables the solutions of the conductivity equation to remain close to the mean of the exact response, even when the plate is driven near a resonance or antiresonance. But in many situations the exact driving-point impedance will not be known; moreover, at very high-frequencies the impedance of nominally identical plates will exhibit statistical variations due to unmodelled or uncertain parameters.

In more general cases of plate excitation, the plate response consists of contributions from both the direct and reverberant fields. In the previous section it was noted that the conductivity model (15) is only applicable for fields made up of propagating plane waves, such as are found in highly reverberant plates. When the direct field produced by a point source participates significantly in the response, equation (15) has been found to perform poorly. The approach taken in this study is to determine the energy distribution for each field separately. The distribution in the direct field is obtained from the known result for an infinite plate; the distribution in the reverberant field is obtained from a homogenous diffuse-field equation similar to equation (15) with a boundary condition corresponding to the direct-field intensity reflected at the boundary. Approximations are introduced to make the method more readily applicable to rectangular plates, but the basic approach is suitable for plates of arbitrary shape.

3.1. DIRECT FIELD ENERGY DISTRIBUTION

The energy distribution in the far-field of a point-excited infinite plate is governed by the following equation [5]:

$$\mathrm{d}/\mathrm{d}r(r\langle e_d\rangle) + (\eta\omega/c)(r\langle e_d\rangle) = 0, \tag{20}$$

where $\langle e_d\rangle$ is the time-averaged energy density in the direct field, and r is the radial distance from the excitation. By applying the appropriate boundary condition at $r = 0$, the solution to this equation can be shown to be

$$\langle e_d\rangle = (P_{in}/2\pi rc)\,\mathrm{e}^{-\alpha r}, \tag{21}$$

where P_{in} is the total input power, and where the diffusion coefficient $\alpha = \omega\eta/c$ is assumed constant across the plate. The intensity in the direct field points radially outward and has a magnitude given by

$$\langle q_d\rangle = c\langle e_d\rangle = (P_{in}/2\pi r)\,\mathrm{e}^{-\alpha r}. \tag{22}$$

Note that equation (21) suggests an infinite energy density at the driving point. This is a result of neglecting the near-field in the vicinity of the excitation. But the driving-point velocity of an infinite plate is known to be

$$v_0 = F_0/8\sqrt{Dm}, \tag{23}$$

where D is the flexural rigidity of the plate, m is the mass/area, and F_0 is the magnitude of the driving point force. This result is equivalent to the frequency average of driving point velocities for a finite plate of similar properties when plotted on a logarithmic scale [18]. The time-average energy density at the driving point therefore becomes

$$\langle e_0\rangle = mv_0^2/2 = F_0^2/128D. \tag{24}$$

The object here is to determine the radius r_0 at which the energy distribution (21) equals the driving point value (24).

Using $P_{in} = F_0^2/16\sqrt{Dm}$ and the approximation $\exp(-\alpha r_0) \simeq 1 - \alpha r_0$ for $\alpha r_0 \ll 1$, and equating (21) and (24), gives the following:

$$(F_0^2/16\sqrt{Dm})([1 - \alpha r_0]/2\pi r_0 c) = F_0^2/128D. \tag{25}$$

The result for r_0 is found to be

$$r_0^{-1} = \pi^2/\lambda + \alpha, \tag{26}$$

where λ is the free-plate flexural wavelength. Within radius r_0, the response can be assumed to be approximately uniform at the driving point value, thus removing the singularity in the energy density function. The energy in the direct field can now be defined with the following piecewise function:

$$\begin{aligned}\langle e_d\rangle &= (P_{in}/2\pi r_0 c)\,\mathrm{e}^{-\alpha r_0}, \qquad 0 < r < r_0,\\ &= (P_{in}/2\pi rc)\,\mathrm{e}^{-\alpha r}, \qquad r > r_0.\end{aligned} \tag{27}$$

3.2. REVERBERANT ENERGY DISTRIBUTION

A reverberant field on a finite plate results from boundary reflection of the direct field. The scattering of cylindrical waves by straight or irregular plate edges produces a field resembling, after a sufficient number of reflections, a diffuse field of plane waves. The reverberant energy is therefore governed by a diffuse equation similar to equation (15) but with the power input term equal to zero:

$$\mathbf{V}^2\overline{\langle e_r\rangle} - \alpha^2\overline{\langle e_r\rangle} = 0, \tag{28}$$

where $\langle e_r \rangle$ is the reverberant energy density and where $\alpha = \omega\eta/c$. For constant α, this equation admits a solution of the form:

$$\overline{\langle e_r \rangle} = A \cosh \alpha x + B \sinh \alpha x + C \cosh \alpha y + D \sinh \alpha y. \tag{29}$$

Power enters the reverberant field at the plate boundary. For a perfectly reflecting boundary, the direct field intensity normal to the boundary must be balanced by the inwardly-directed reverberant intensity. The net intensity crossing the boundary will then be zero, as is required by equation (19). The boundary condition for the reverberant field equation (28) can be stated more generally as

$$(c^2/\omega\eta)\, \nabla \overline{\langle e_r \rangle}|_\Gamma \cdot \mathbf{n} = \rho \langle \mathbf{q}_d \rangle|_\Gamma \cdot \mathbf{n}, \tag{30}$$

where the right side is the proportion of the direct field reflected back to the plate in a direction normal to the boundary, with ρ representing the reflectivity of the boundary. When applied to particular plates the resulting expressions can be quite complicated, thus ruling out a closed form solution of the form (29). However, it is shown in section 4 that analytical solutions for rectangular plates can be obtained by assuming the reflected intensity distribution to be uniform along each boundary segment. Without this approximation, numerical solutions can be found by finite element discretization of equation (28) and by appropriate discretization of the power input at the boundary.

3.3. PARTITION OF INPUT POWER

If it is assumed that no energy leaks to the surroundings, conservation of energy requires that the direct and reverberant fields absorb all input power to the plate. Denoting P_d as the power dissipated in the direct field and P_r as the power absorbed by the reverberant field, it is required that

$$P_{in} = P_d + P_r. \tag{31}$$

Power entering a discrete source point is considered to spread coherently across the plate until it reaches the boundary. The power absorbed in the direct field is just that portion of input power dissipated in the coherent wave field; the remainder reaches the boundary and thereafter is absorbed in the reverberant field.

In general it is difficult to determine the power dissipation in the direct field. The integral to be evaluated is

$$P_d = \int_A \frac{\omega\eta P_{in}}{2\pi r c}\, \mathrm{e}^{-\alpha r}\, \mathrm{d}A, \tag{32}$$

which only has a closed form solution in exceptional cases. If the source point is located near the centre of the plate, a useful approximation is to compute expression (32) assuming a circular plate with an equivalent surface area. Denoting the radius of the equivalent plate as $R = \sqrt{A/\pi}$, the integral evaluates as

$$P_d = P_{in}(1 - \mathrm{e}^{-\alpha R}). \tag{33}$$

Comparing to equation (31) gives

$$P_r = P_{in}\, \mathrm{e}^{-\alpha R}. \tag{34}$$

Because the direct field concentrates energy (and therefore dissipates energy) near the excitation point, the circular plate approximation will be quite accurate as long as the source is at least a few wavelengths from the plate edge. With heavy damping or with short wavelength vibration $\alpha R \gg 1$, and nearly all the input power is absorbed in the direct field.

In this case, the reverberant field will make a negligible contribution to the energy and the plate behaves as though it were infinite. With light damping or long wavelength vibration, $\alpha R \ll 1$, and nearly all the power is transferred to the reverberant field. In this case the direct field will make a negligible contribution to the energy, and the problem can be sufficiently well analyzed with the standard conductivity method or SEA. The hybrid energy method provides the link between these two extreme cases, and is therefore especially useful in the situations where $\alpha R \sim 1$.

4. APPLICATION TO RECTANGULAR PLATES

Consider the rectangular plate in Figure 1 in which a point harmonic load is applied at location (x_0, y_0). The contribution from the direct field is given by equation (27) with a radial distance of $r = [(x - x_0)^2 + (y - y_0)^2]^{1/2}$. The contribution from the reverberant field is obtained from equation (28) with a boundary condition determined by substituting equation (22) into the right-hand side of equation (30). A reflectivity $\rho = 1$ is assumed for all four edges. Hence the boundary condition at the edge $x = a$ becomes

$$(c^2/\omega\eta)(\partial\overline{\langle e_r \rangle}/\partial x)|_{x=a} = (P_{in}(a - x_0)/2\pi)\exp(-\alpha\sqrt{(a - x_0)^2 + (y - y_0)^2}) \\ /[(a - x_0)^2 + (y - y_0)^2], \tag{35}$$

which ensures that the net intensity, given by the sum of the intensities in the direct and reverberant fields, is zero across this edge. As a solution of the form (29) is unable to satisfy this boundary condition, a convenient simplification is to replace the distribution on the right side of equation (35) with a constant value consistent with the total power reflected at the boundary and with the proximity of the point source to each of the plate edges.

One way to do this is to specify for each boundary segment a value in proportion to the maximum normal intensity. Along the edge $x = a$ the maximum intensity occurs at $y = y_0$ and is given by

$$Q_1 = (P_{in}/2\pi)(e^{-\alpha(a - x_0)}/[a - x_0]). \tag{36}$$

Likewise the maximum intensities along edges 2, 3 and 4, respectively, are found to be

$$Q_2 = \frac{P_{in}\, e^{-\alpha x_0}}{2\pi x_0}, \qquad Q_3 = \frac{P_{in}\, e^{-\alpha(b - y_0)}}{2\pi(b - y_0)}, \qquad Q_4 = \frac{P_{in}\, e^{-\alpha y_0}}{2\pi y_0}. \tag{37}$$

The boundary conditions for the four segments can now be stated approximately as

$$(c^2/\omega\eta)\nabla\overline{\langle e_r \rangle} \cdot \mathbf{n}|_{\Gamma_i} = \beta Q_i, \tag{38}$$

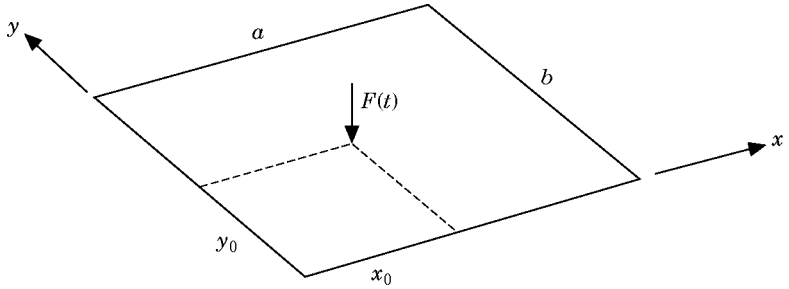

Figure 1. Rectangular plate with point force excitation.

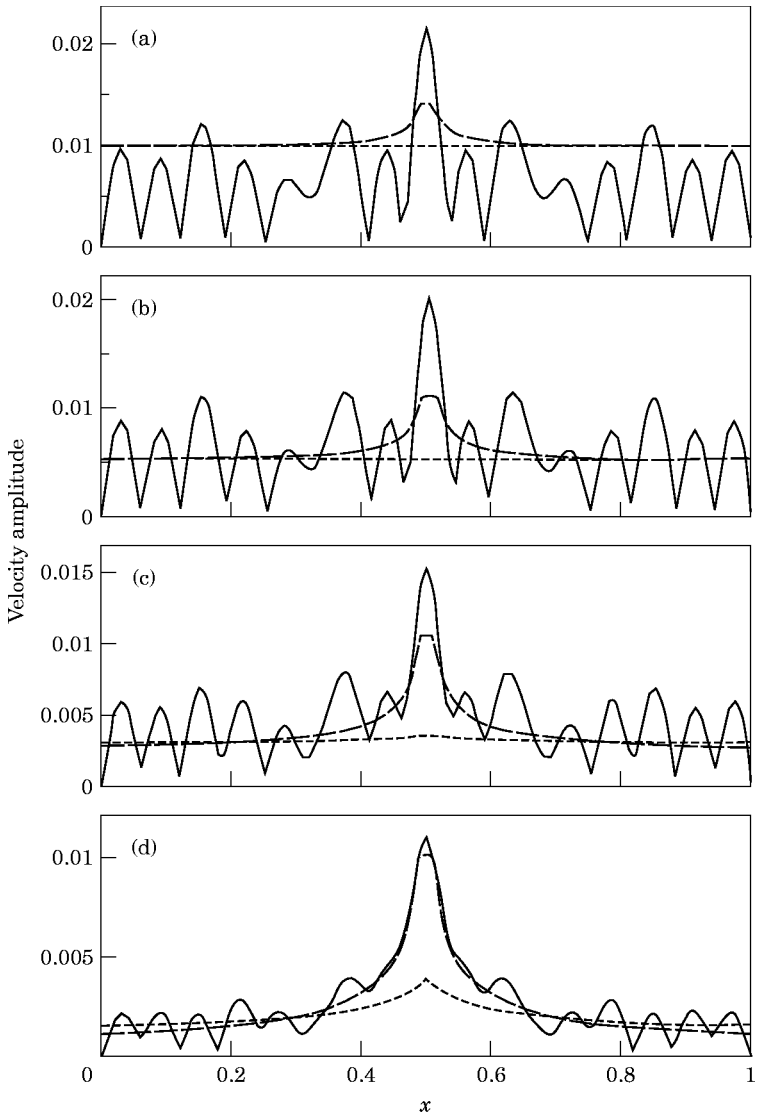

Figure 2. Velocity amplitude (m/s) along an axis passing through the centre of a square plate, harmonic excitation: —, biharmonic plate equation; — —, hybrid model; --, conductivity model. (a) $\eta = 0{\cdot}003$; (b) $\eta = 0{\cdot}01$; (c) $\eta = 0{\cdot}03$; (d) $\eta = 0{\cdot}1$.

where β is a constant of proportionality. Integrating the reflected intensity around the perimeter of the plate gives the total power transferred to the reverberant field:

$$P_r = \beta b(Q_1 + Q_2) + \beta a(Q_3 + Q_4). \tag{39}$$

Substituting the expression for P_r from equation (34), the following expression for β is obtained:

$$\beta = P_{in}\, \mathrm{e}^{-\alpha R}/[b(Q_1 + Q_2) + a(Q_3 + Q_4)]. \tag{40}$$

With the scale factor β and the simplified edge functions (36, 37), an analytical solution in the form (29) can now be found which satisfies the boundary conditions in equation (38). The resulting coefficients are

$$A = \beta(Q_1 + Q_2 \cosh(\alpha a))/c \sinh(\alpha a), \qquad B = -\beta Q_2/c,$$

$$C = \beta(Q_3 + Q_4 \cosh(\alpha b))/c \sinh(\alpha b), \qquad D = -\beta Q_4/c. \tag{41}$$

In situations where the reverberant field makes a large contribution to the total energy, its distribution tends to be nearly uniform. This is equivalent to the case of low damping or long wavelength in which $\alpha a \ll 1$ and $\alpha b \ll 1$. In these limits, the reverberant response function (29) reduces to

$$\overline{\langle e_r \rangle} \simeq A + C \simeq (\beta/c\alpha ab)[b(Q_1 + Q_2) + a(Q_3 + Q_4)] = P_r/\omega\eta ab, \tag{42}$$

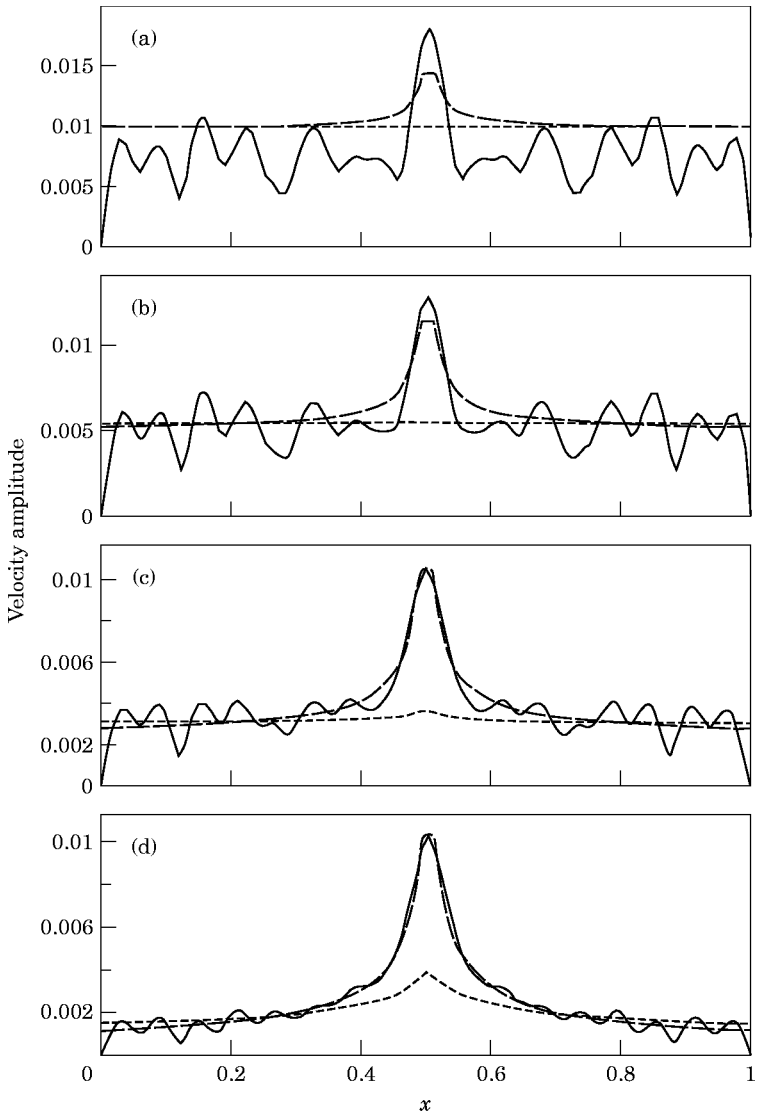

Figure 3. Velocity amplitude (m/s) along an axis passing through the centre of a square plate, 1/3 octave band excitation: —, biharmonic plate equation; ——, hybrid model; --, conductivity model. (a) $\eta = 0{\cdot}003$; (b) $\eta = 0{\cdot}01$; (c) $\eta = 0{\cdot}03$; (d) $\eta = 0{\cdot}1$.

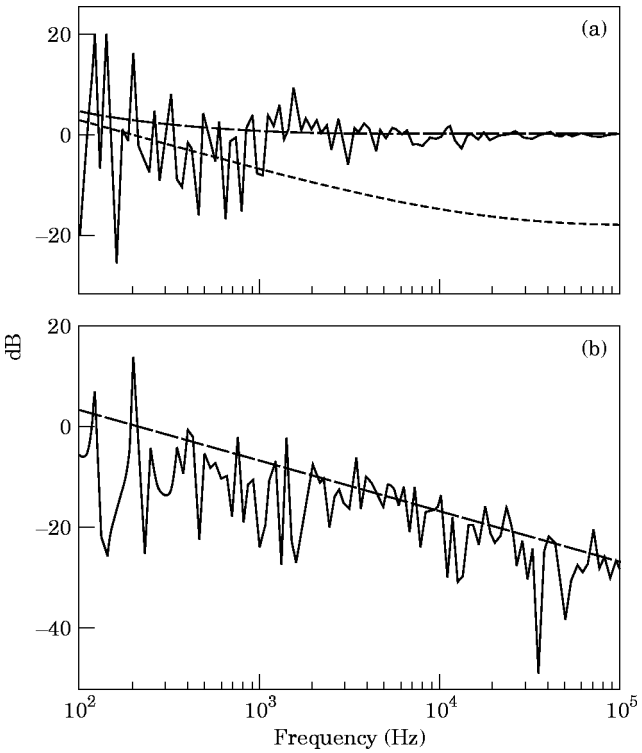

Figure 4. Frequency response of a 1 m square plate at (a) the driving point, and (b) position $x = 0{\cdot}75$, $y = 0{\cdot}5$, for centre harmonic loading and $\eta = 0{\cdot}01$: —, biharmonic plate equation; ——, hybrid model; --, conductivity model.

which is identical to the result obtained from SEA theory when $P_r = P_{in}$. Note, however, that this constant value does not satisfy the homogeneous equation for the reverberant field, equation (28). Instead, it is the first term in a Fourier series expansion of the particular solution to the non-homogeneous conductivity equation (15).

The total energy distribution is obtained by summing the direct and reverberant field contributions:

$$\overline{\langle e \rangle} = \langle e_d \rangle + \overline{\langle e_r \rangle}. \tag{43}$$

Since average energy density is just twice the average kinetic energy, the RMS velocity is

$$v_{RMS} = \sqrt{\frac{\overline{\langle e \rangle}}{m}}, \tag{44}$$

where m is the mass per unit area of plate. Similarly, the net intensity on the plate is just the sum of the direct-field and reverberant components:

$$\overline{\langle \mathbf{q} \rangle} = \langle \mathbf{q}_d \rangle + \overline{\langle \mathbf{q}_r \rangle}, \tag{45}$$

where the magnitude of $\langle \mathbf{q}_d \rangle$ is given by equation (22), and where $\overline{\langle \mathbf{q}_r \rangle}$ is found to be

$$\overline{\langle \mathbf{q}_r \rangle} = -c^2/\omega\eta \, \nabla \overline{\langle e_r \rangle} = -c(A \sinh \alpha x + B \sinh \alpha x)\mathbf{i} - c(C \sinh \alpha y + D \cosh \alpha y)\mathbf{j}. \tag{46}$$

The hybrid model can also be applied to plates with multiple point sources simply by summing the energy distribution produced by each source on its own. In doing so it is implicitly assumed that the forces are uncorrelated either in time, by having different frequencies or phases, or in space, by being separated at distances significantly larger than the flexural wavelength [19]. An example of a rectangular plate excited by two forces is given in section 4.2.

4.1. SQUARE PLATE WITH CENTRAL LOADING

The hybrid model is now tested on a square plate with dimension $a = b = 1$ m, and a thickness of 1 mm. A harmonic point force of unit amplitude and a frequency of 700 Hz is applied at the centre of the plate. The results are compared with those of two other methods: the conductivity method in which equation (15) is used with an input power distribution given by

$$\pi_i = P_{in}\delta(x - x_0)\delta(y - y_0), \tag{47}$$

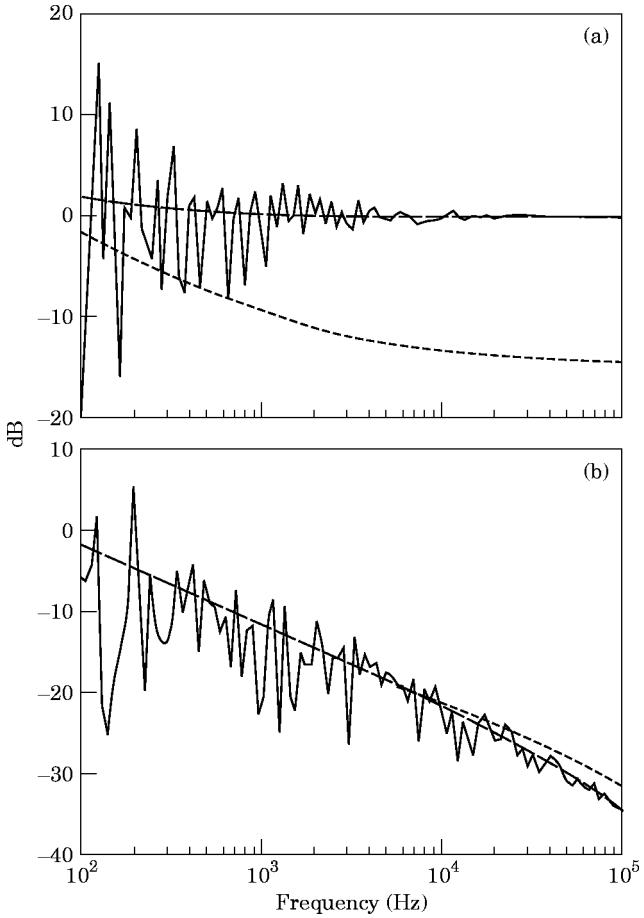

Figure 5. Frequency response of a 1 m square plate at (a) the driving point, and (b) position $x = 0{\cdot}75$, $y = 0{\cdot}5$, for centre harmonic loading and $\eta = 0{\cdot}03$: —, biharmonic plate equation; — —, hybrid model; --, conductivity model.

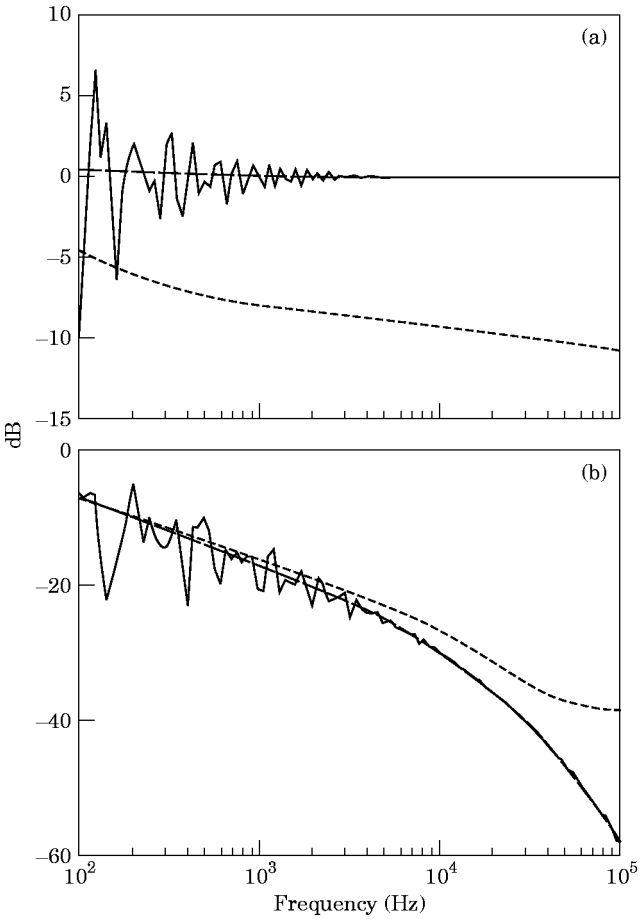

Figure 6. Frequency response of a 1 m square plate at (a) the driving point, and (b) position $x = 0{\cdot}75$, $y = 0{\cdot}5$, for centre harmonic loading and $\eta = 0{\cdot}10$: —, biharmonic plate equation; — —, hybrid model; --, conductivity model.

and a solution is determined using a Fourier series expansion satisfying the boundary conditions (19); also compared is an "exact" solution obtained from Fourier series analysis of the biharmonic plate equation, assuming simply-supported boundary conditions.

Velocity response profiles obtained with three different methods are shown in Figure 2 for four different loss factors. The profiles are taken from a line passing through the excitation, parallel to the coordinate axes. Two parameters that strongly affect the accuracy of the two energy methods (i.e., the conductivity and hybrid methods) are the input power estimate and the loss factor. In the results presented here, input power has been calculated for an equivalent infinite plate; consequently, the overall level predicted by the energy models may be too high or too low depending on whether the input power has been overestimated or underestimated. If at the chosen frequency the plate is near resonance, the actual input impedance is very small and hence the input power very large in comparison to the infinite plate value. Conversely, near an antiresonance the actual input power is small compared to the infinite-plate value and the response level will be overestimated.

Figures 2(a) and (b) show clearly the effect of loss factor on the results. Although the exact response is very similar in these two figures, the response level predicted by the two energy models away from the driving point is twice as high as for $\eta = 0{\cdot}003$ as it is for $\eta = 0{\cdot}01$. The response profiles for the energy models are essentially flat, except near the driving point in the hybrid model, indicating the dominance of the reverberant field at low damping. The large variation with loss factor is reflected in the denominator of the limiting solution (42) for low damping.

In Figures 2(c) and (d), profiles for the two higher loss factors are given in which a significant difference in the two energy models may be observed. In this range of damping, both the direct and reverberant fields make significant contributions to the vibration. As the loss factor increases, the improvement in the region of the excitation is readily observed. Note that the driving point value in the direct field is evaluated at radius r_0 given by equation (26), and is constant in the region $r < r_0$. The value does not match up with the true driving point velocity because equation (26) was derived assuming that all input power is absorbed in the direct field, an assumption which is justifiable only at the higher loss factors. It is evident that as the damping increases and the finite plate behaves more and more like an infinite plate, the driving point velocity predicted by the hybrid model gradually approaches the true mean value.

In Figure 3 the energy modelling results of Figure 2 are compared with the plate velocity under 1/3 octave band excitation. The latter was calculated by averaging harmonic responses at 80 frequencies distributed throughout a band centred at 700 Hz. The basic features of the plots are the same as those observed for harmonic loading. The sharpness of the standing wave pattern is reduced with this type of excitation, revealing a closer match between the exact and energy modelling results.

To assess how the hybrid model performs over a wide range of excitation frequencies, the responses of two points in the structure—the driving point (0, 0) and a point midway

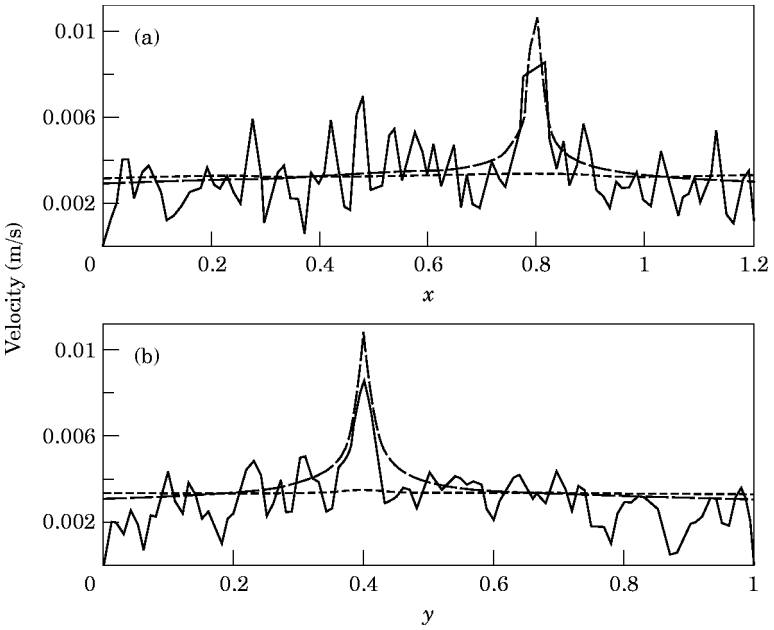

Figure 7. Velocity amplitude (m/s) for a rectangular plate with two forces, $\eta = 0.01$: (a) $y = 0.4$; (b) $x = 0.8$; —, biharmonic plate equation; ——, hybrid model; --, conductivity model.

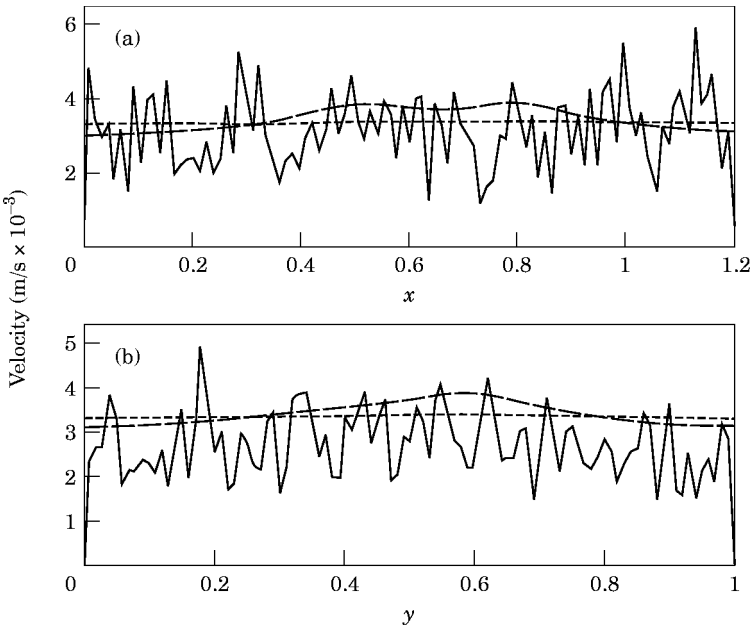

Figure 8. Velocity amplitude (m/s) for a rectangular plate with two forces, $\eta = 0.01$: (a) $y = 0.5$; (b) $x = 0.6$; ——, biharmonic plate equation; — — hybrid model; --, conductivity model.

between the driving point and the plate edge $(a/2, 0)$—are given in Figures 4–6 as a function of frequencies. At the midway point, the energy models give similar velocities except at high frequencies and high loss factors. The average response level is predicted

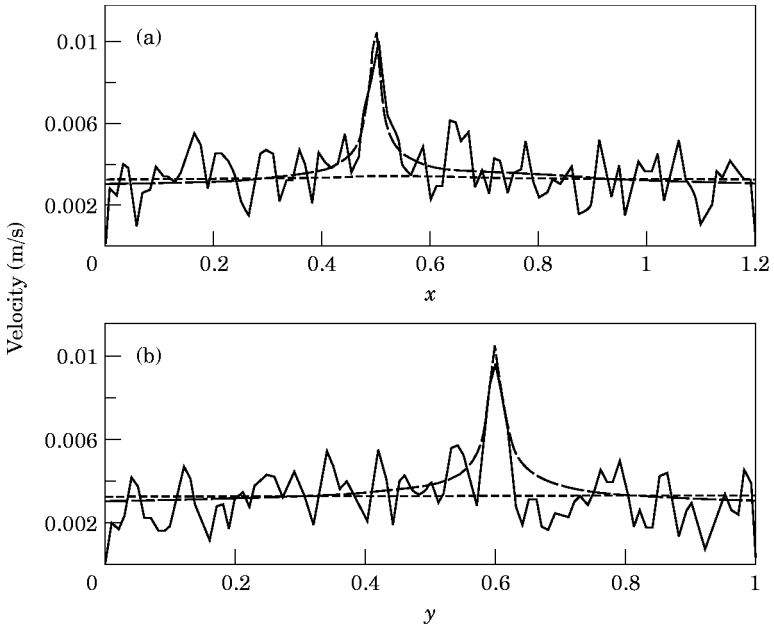

Figure 9. Velocity amplitude (m/s) for a rectangular plate with two forces, $\eta = 0.01$: (a) $y = 0.6$; (b) $x = 0.5$; ——, biharmonic plate equation; — —, hybrid model; --, conductivity model.

quite closely, with the hybrid model being somewhat more accurate at high frequency. The plots for the driving point illustrate a profound difference between the two energy models. Note that when plotted on the logarithmic scale, the average driving point velocity is invariant with frequency, and is equivalent to the driving-point velocity of an infinite plate (23). This value is chosen as the reference point for the plots. The conductivity model generally predicts a driving point velocity which is too small, and which falls to -10 dB or less at high frequency. On the other hand the hybrid model gives a driving-point value which approaches the mean value monotonically from above at all the levels of damping that have been tested. The error can be seen to increase with decreasing frequency and loss factor, but it is never more than a small fraction of the local resonance peak.

4.2. RECTANGULAR PLATE EXCITED BY TWO POINT FORCES

The same comparison of methods is now performed for a rectangular plate with dimensions $a = 1{\cdot}2$ m and $b = 1$ m, and thickness 1 mm. Two harmonic forces of unit amplitude are applied at locations (0·8, 0·4) and (0·5, 0·6), with excitation frequencies of 3000 and 3300 Hz, respectively. Figures 7–9 give velocity response profiles at several locations and for a loss factor of 0·01. Results for the two energy methods were obtained

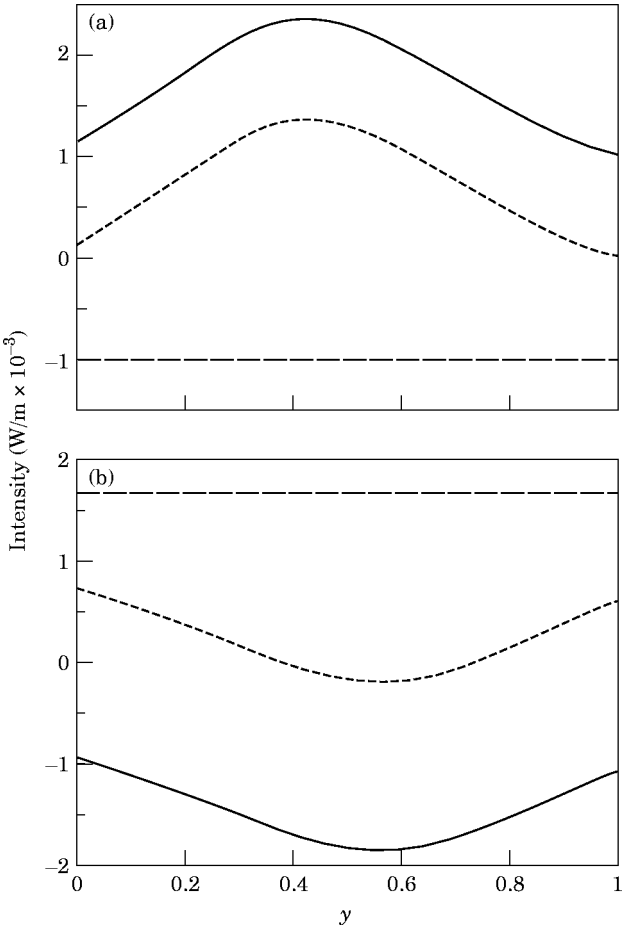

Figure 10. Normal intensity (W/m) along edges of a rectangular plate, $\eta = 0.01$: (a) $x = a$; (b) $x = 0$; ——, direct field intensity: — —, reverberant field intensity; --, direct plus reverberant intensity.

by adding the energy fields produced by each force separately. For the "exact" results, the velocity amplitudes calculated for each force could not be directly added because of their differing time dependencies. The displayed velocity is instead the square root of the mean squares summed. As in the square plate example, the hybrid model results follow the shape of the exact response much more closely near the driving points than do the results of the conductivity model. Moreover, the overall velocity levels are more accurate than in the previous example with this amount of damping (Figure 2(b)), primarily because of the increase in frequency. Input power to the plate due to each excitation was again calculated assuming an infinite plate, an approximation which here produces very satisfactory results.

A consequence of approximating the edge functions is that a zero net intensity across the boundary is not exactly maintained at each boundary point. Figure 10(a) shows the intensity in the x direction across the edge $x = a$ in the direct and reverberant fields. The direct field intensity is calculated with the right side of equation (35), and is seen here to be positive, indicating that energy is flowing away from the plate. The reverberant intensity is determined by scaling the maximum intensity in the direct field along this edge, and it is shown here to be negative, indicating that energy is reflected back into the plate. The sum of the two is non-zero except at just one location on the edge, and overall is more positive than negative, indicating a net flow out of the plate. On the other hand the results for the edge $x = 0$ (Figure 10(b)) show a net flow of energy into the plate. The hybrid model satisfies not a local, but a global boundary condition requiring the total intensity out of the plate to be approximately zero, the approximation arising from the circular plate assumption in section 3.3. The actual deviation in the intensity at the boundary is small in comparison to the intensity near the excitations, as can be seen in Figure 11. Away from the driving points the intensity drops rapidly, mainly due to spreading of energy in the direct field. But significant velocity levels can still occur in regions of low intensity, as can be observed in Figures 7–9.

Finally, it should be noted that the uniform approximation to the edge functions was needed only in order to use the analytical solution given by equations (29) and (41); if a finite element implementation of the hybrid model were used, the non-uniform edge distributions could then be applied. However, the results presented here indicate that approximating the edge functions makes very little difference to the overall velocity, and is not as nearly an important factor in the analysis as is accurately estimating the total input power to the system and the power transferred to the reverberant field.

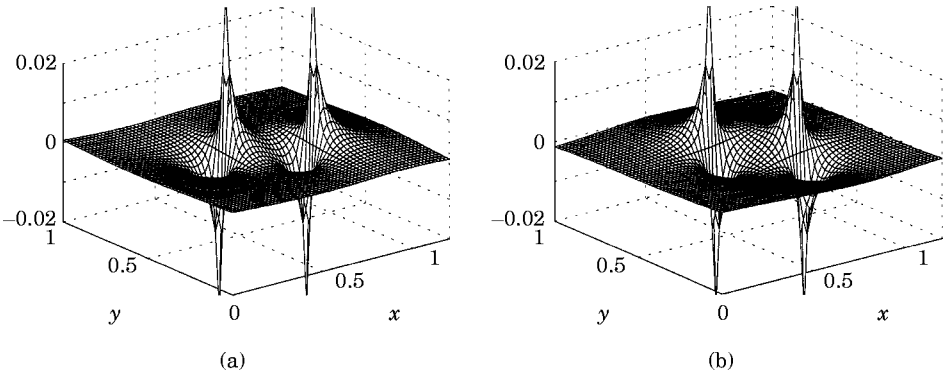

Figure 11. Intensity distribution (W/m) in a rectangular plate obtained with a hybrid conductivity model, $\eta = 0.01$: (a) q_x; (*b*) q_y.

5. CONCLUSION

This paper has described the use of a hybrid energy method for predicting the high frequency vibratory response of point-loaded plates. The method is proposed as an improvement to the conductivity method for the general class of point-loaded plates. The diffuse-field equation derived in section 2, which forms the basis of the conductivity method, assumes a randomly directed plane wave field. This equation is therefore unsuitable for plate applications in which a significant direct field is generated by the loading.

The hybrid method presented in this study takes separate account of the direct and reverberant fields produced by the excitation: the former through the known result for an infinite plate, and the latter through a homogeneous conductivity equation with an appropriate reflected power distribution at the boundary. The power transferred to the reverberant field is estimated assuming a circular plate of equivalent area. In developing the method, attention is focussed on rectangular plates with perfectly reflective boundaries, although the method can be generalized to irregularly shaped plates and only partially reflective boundaries.

Examples of a centrally-loaded square plate and a rectangular plate with two point forces show that the hybrid modelling technique improves the response prediction as damping increases, or as the wavelength decreases relative to the size of the plate. For low values of damping in which the plate response is almost totally reverberant, the hybrid method performs in a manner very similar to the conductivity method and SEA.

The hybrid method is suitable only for point-excited plates in which the driving point is not less than a few wavelengths from the plate edge. The method has the advantage of being computationally simple. The direct field distribution is by definition known explicitly. It was also shown that if the plate is rectangular and the reflected power distribution along each segment of the boundary is assumed uniform, a closed-form solution for the reverberant energy field is available. Thus for known input power, dimensions, and loss factor of a point-loaded rectangular plate, the response can be calculated directly, without recourse to numerical analysis or solutions involving series expansions. In this sense the method is similar to SEA. But it differs in being able to predict, often with great accuracy, the spatial variation of the plate response. The conductivity model is also capable of predicting the spatial variation of the response, but generally does so with less accuracy. Moreover, solutions with that method are only obtained using Fourier series analysis or a numerical method such as finite element discretization. Thus, with respect to both accuracy and computational simplicity, the hybrid method is a significant advance in the energy modelling of point-loaded plates. It should be noted that although the closed form solutions for the direct and reverberant fields, equations (21) and (29), are only valid with a constant value of the diffusion parameter α, the governing equations for the two fields can still be applied in cases of non-uniform plates, or plates with spatial varying distributions of damping material.

ACKNOWLEDGMENT

This research was supported through the Industrial Research Fellowship program of the Natural Sciences and Engineering Research Council of Canada.

REFERENCES

1. D. J. Nefske and S. H. Sung 1989 *Journal of Vibration, Acoustics, Stress, and Reliability in Design* **111**, 94–100. Power flow finite element analysis of dynamic systems: basic theory and application to beams.

2. J. C. Wohlever and R. J. Bernhard 1992 *Journal of Sound and Vibration* **153**, 1–19. Mechanical energy flow models of rods and beams.
3. P. Cho 1993 *Ph.D. Thesis*, *Purdue University*. Energy flow analysis of coupled structures.
4. L. E. Buvailo and A. V. Ionov 1980 *Soviet Physics—Acoustics* **26**, 277–279. Application of the finite element method to the investigation of the vibroacoustical characteristics of structures at high audio frequencies.
5. O. M. Bouthier 1992 *Ph.D. Thesis*, *Purdue University*. Energetics of vibrating systems.
6. O. M. Bouthier and R. J. Bernhard 1992 *American Institute of Aeronautics and Astronautics Journal* **30**, 616–623. Models of space-averaged energetics of plates.
7. O. M. Bouthier and R. J. Bernhard 1995 *Journal of Sound and Vibration* **182**, 129–147. Simple models of energy flow in vibrating membranes.
8. O. M. Bouthier and R. J. Bernhard 1995 *Journal of Sound and Vibration* **182**, 149–164. Simple models of the energetics of transversely vibrating plates.
9. R. J. Bernhard and J. E. Huff Jr 1995 *DE-Vol*. 84-2, *ASME Design Engineering Technical Conferences* **3**, Part B, 565–576. Structural-acoustic design at high frequency using the energy finite element method.
10. J. E. Huff Jr and R. J. Bernhard 1995 *Proceedings of Internoise* 95, 1221–1226. Prediction of high frequency vibrations in coupled plates using energy finite elements.
11. S. C. Burrell, J. L. Warner and M. W. Chernuka 1990 *Paper* 90-*WA*/*NCA*-10, *ASME Winter Annual Meeting*. Power flow finite element analysis applied to a thin circular plate.
12. H. S. Kim, H. J. Kang, and J. S. Kim 1994 *Journal of Sound and Vibration* **174**, 493–504. A vibration analysis of plates at high frequencies by the power flow method.
13. R. S. Langley 1995 *Journal of Sound and Vibration* **184**, 637–657. On the vibrational conductivity approach to high frequency dynamics for two-dimensional structural components.
14. A. Carcaterra and A. Sestieri 1995 *Journal of Sound and Vibration* **188**, 269–282. Energy density equations and power flow in structures.
15. Y. Lase and L. Jezequel 1990 *Proceedings of the* 3*rd International Congress on Intensity Techniques* 145–150. Analysis of a dynamic system based on a new energetic formulation.
16. L. Cremer and M. Heckl 1988 *Structure-Borne Sound* (Second edition). New York: Springer-Verlag.
17. D. U. Noiseux 1970 *Journal of Acoustical Society of America* **47**, 238–247. Measurement of power flow in uniform beams and plates.
18. E. Skudrzyk 1980 *Journal of Acoustical Society of America* **67**, 1105–1135. The mean-value method of predicting the dynamic response of complex vibrators.
19. E. H. Dowell and Y. Kubota 1985 *Journal of Applied Mechanics* **52**, 949–957. Asymptotic modal analysis and statistical energy analysis of dynamical systems.